Electronic Supporting Information Materials

Synthesis and anticancer mechanisms of four novel platinum(II) 4′-substituted-2,2′:6′,2″-terpyridine complexes

Chun-Jie Liang,‡[a] Run-Chun Wu,‡[a] Xiao-Qiong Huang,‡[a] Qi-Pin Qin,*[a] Hong Liang[b] and Ming-Xiong Tan*[a]

Table S1. Crystal data and structure refinement for PtS.

Empirical formula	$C_4H_{12}Cl_2O_2PtS_2$
Formula weight	422.25
Temperature/K	150.0
Crystal system	monoclinic
Space group	$P2_1/n$
a/Å	8.6224(5)
b/Å	13.5614(6)
c/Å	9.3946(5)
α/°	90
β/°	105.6469(19)
γ/°	90
Volume/Å^3	1057.82(10)
Z	4
ρ_{calc}mg/mm^3	2.651
m/mm^{-1}	14.119
F(000)	784.0
Crystal size/mm^3	0.24 × 0.24 × 0.23
2Θ range for data collection	5.414 to 49.994°
Index ranges	$-10 \le h \le 10$, $-16 \le k \le 16$, $-11 \le l \le 11$
Reflections collected	21981
Independent reflections	1858[R(int) = 0.0501]
Data/restraints/parameters	1858/0/105
Goodness-of-fit on F^2	1.003
Final R indexes [I>=2σ (I)]	R_1 = 0.0223, wR_2 = 0.0586
Final R indexes [all data]	R_1 = 0.0236, wR_2 = 0.0593
Largest diff. peak/hole / e Å^{-3}	1.73/-1.11

Table S2. Bond Lengths for PtS.

Atom	Atom	Length/Å	Atom	Atom	Length/Å
Pt1	S2	2.2312(12)	S2	C3	1.775(5)
Pt1	Cl1	2.3221(13)	S2	C4	1.775(5)

Pt1	S1	2.2478(13)	S1	O1	1.470(4)
Pt1	Cl2	2.3150(15)	S1	C2	1.781(5)
S2	O2	1.466(4)	S1	C1	1.771(5)

Table S3. Bond Angles for PtS.

Atom	Atom	Atom	Angle/°	Atom	Atom	Atom	Angle/°
S2	Pt1	Cl1	176.09(5)	C3	S2	Pt1	108.2(2)
S2	Pt1	S1	91.11(5)	C3	S2	C4	102.8(3)
S2	Pt1	Cl2	88.65(5)	C4	S2	Pt1	111.5(2)
S1	Pt1	Cl1	92.73(5)	O1	S1	Pt1	112.81(16)
S1	Pt1	Cl2	174.95(5)	O1	S1	C2	108.0(2)
Cl2	Pt1	Cl1	87.46(5)	O1	S1	C1	109.8(2)
O2	S2	Pt1	117.39(16)	C2	S1	Pt1	113.16(18)
O2	S2	C3	108.0(3)	C1	S1	Pt1	112.12(19)
O2	S2	C4	107.9(3)	C1	S1	C2	100.2(3)

Table S4. Crystal data and structure refinement for tpy1Pt.

Empirical formula	$C_{30}H_{38}Cl_4N_6O_5Pt_2S_2$
Formula weight	1158.76
Temperature/K	150.0
Crystal system	triclinic
Space group	P-1
a/Å	9.7407(6)
b/Å	11.1975(5)
c/Å	19.3778(12)
α/°	77.3037(18)
β/°	79.196(2)
γ/°	75.1122(17)
Volume/Å^3	1973.3(2)
Z	2
ρ_{calc}mg/mm^3	1.950
m/mm^{-1}	7.502
F(000)	1112.0
Crystal size/mm^3	0.26 × 0.25 × 0.21
2Θ range for data collection	4.352 to 50.02°
Index ranges	$-11 \le h \le 11$, $-13 \le k \le 13$, $-23 \le l \le 23$
Reflections collected	60448
Independent reflections	6956[R(int) = 0.0821]
Data/restraints/parameters	6956/294/448
Goodness-of-fit on F^2	1.125
Final R indexes [I>=2σ (I)]	R_1 = 0.0550, wR_2 = 0.1383
Final R indexes [all data]	R_1 = 0.0638, wR_2 = 0.1446

Largest diff. peak/hole / e Å^{-3}	2.87/-3.56

Table S5. Bond Lengths for tpy1Pt.

Atom	Atom	Length/Å	Atom	Atom	Length/Å
Pt1	Cl1	2.297(3)	N6	C24	1.477(14)
Pt1	S1	2.213(3)	N6	C20	1.465(14)
Pt1	Cl2	2.297(3)	N3	C5	1.316(13)
Pt1	N1	2.072(9)	N3	C9	1.346(13)
Pt2	Cl3	2.305(3)	C11	C10	1.402(15)
Pt2	Cl4	2.291(3)	C23	C22	1.563(16)
Pt2	S2	2.219(3)	C23	C24	1.516(17)
Pt2	N4	2.097(9)	C22	C25	1.490(18)
S1	O1	1.467(9)	C1	C2	1.386(15)
S1	C26	1.773(13)	C7	C8	1.397(14)
S1	C27	1.754(13)	C7	C6	1.400(14)
S2	O2	1.464(10)	C7	C14	1.481(14)
S2	C29	1.764(15)	C12	C13	1.365(16)
S2	C28	1.770(14)	C8	C9	1.392(14)
N4	C11	1.340(14)	C17	C18	1.385(14)
N4	C12	1.340(14)	C17	C16	1.400(15)
N1	C1	1.349(13)	C6	C5	1.396(14)
N1	C4	1.344(14)	C15	C16	1.376(15)
C21	C22	1.518(17)	C15	C14	1.399(14)
C21	C20	1.519(17)	C4	C3	1.379(15)
N5	C13	1.344(14)	C18	C19	1.376(15)
N5	C10	1.320(13)	C2	C5	1.505(14)
N2	C2	1.337(14)	C14	C19	1.389(15)
N2	C3	1.327(13)	C9	C10	1.483(14)
O3	C25	1.296(17)	C25	O4	1.231(17)
N6	C17	1.431(12)	O5	C30	1.38(2)

Table S6. Bond Angles for tpy1Pt.

Atom	Atom	Atom	Angle/°	Atom	Atom	Atom	Angle/°
Cl1	Pt1	Cl2	178.50(10)	C25	C22	C21	114.8(11)
S1	Pt1	Cl1	94.19(11)	C25	C22	C23	107.9(10)
S1	Pt1	Cl2	87.09(11)	N1	C1	C2	120.1(10)
N1	Pt1	Cl1	89.0(3)	C8	C7	C6	115.6(9)
N1	Pt1	S1	176.4(3)	C8	C7	C14	123.3(9)
N1	Pt1	Cl2	89.8(3)	C6	C7	C14	121.0(9)
Cl4	Pt2	Cl3	176.94(12)	N4	C12	C13	121.0(10)
S2	Pt2	Cl3	85.79(11)	C9	C8	C7	120.0(9)
S2	Pt2	Cl4	93.31(12)	C18	C17	N6	121.0(10)
N4	Pt2	Cl3	91.7(2)	C18	C17	C16	119.3(9)

N4	Pt2	Cl4	89.5(3)	C16	C17	N6	119.7(9)
N4	Pt2	S2	174.5(2)	C5	C6	C7	120.3(9)
O1	S1	Pt1	117.7(4)	C16	C15	C14	122.5(10)
O1	S1	C26	107.0(7)	N1	C4	C3	119.6(10)
O1	S1	C27	108.4(6)	C19	C18	C17	119.5(10)
C26	S1	Pt1	113.8(5)	N2	C2	C1	121.9(9)
C27	S1	Pt1	107.0(4)	N2	C2	C5	117.8(9)
C27	S1	C26	101.7(6)	C1	C2	C5	120.1(9)
O2	S2	Pt2	116.7(4)	C15	C16	C17	119.5(9)
O2	S2	C29	107.1(7)	N2	C3	C4	123.2(10)
O2	S2	C28	109.5(7)	C15	C14	C7	121.7(9)
C29	S2	Pt2	114.3(5)	C19	C14	C7	122.3(9)
C29	S2	C28	101.9(7)	C19	C14	C15	116.0(9)
C28	S2	Pt2	106.3(5)	N3	C5	C6	123.7(9)
C11	N4	Pt2	117.7(7)	N3	C5	C2	116.5(9)
C11	N4	C12	116.7(9)	C6	C5	C2	119.8(9)
C12	N4	Pt2	125.3(7)	N3	C9	C8	123.6(9)
C1	N1	Pt1	120.7(7)	N3	C9	C10	116.3(9)
C4	N1	Pt1	121.0(7)	C8	C9	C10	120.1(9)
C4	N1	C1	118.3(9)	N5	C13	C12	123.3(10)
C22	C21	C20	111.3(10)	N5	C10	C11	121.6(10)
C10	N5	C13	116.0(9)	N5	C10	C9	120.2(9)
C3	N2	C2	116.7(9)	C11	C10	C9	118.2(9)
C17	N6	C24	118.4(8)	C18	C19	C14	123.2(10)
C17	N6	C20	120.2(8)	N6	C24	C23	110.3(9)
C20	N6	C24	109.4(8)	N6	C20	C21	110.7(9)
C5	N3	C9	116.8(9)	O3	C25	C22	115.6(12)
N4	C11	C10	121.4(10)	O4	C25	O3	122.3(14)
C24	C23	C22	111.2(10)	O4	C25	C22	121.6(13)
C21	C22	C23	110.2(10)				

Table S7. Crystal data and structure refinement for tpy2Pt.

Empirical formula	$C_{24}H_{25}Cl_4N_5O_2Pt_2S$
Formula weight	979.53
Temperature/K	150.0
Crystal system	triclinic
Space group	P-1
a/Å	11.4487(5)
b/Å	11.5208(6)
c/Å	12.9041(7)
α/°	105.599(2)
β/°	108.6990(10)
γ/°	108.5620(10)
Volume/Å^3	1391.80(12)

Z	2
ρ_{calc}mg/mm^3	2.337
m/mm^{-1}	10.533
F(000)	920.0
Crystal size/mm^3	0.23 × 0.22 × 0.20
2Θ range for data collection	4.096 to 50.198°
Index ranges	-13 ≤ h ≤ 13, -13 ≤ k ≤ 13, -15 ≤ l ≤ 15
Reflections collected	37606
Independent reflections	4968[R(int) = 0.0534]
Data/restraints/parameters	4968/0/347
Goodness-of-fit on F^2	1.008
Final R indexes [I>=2σ (I)]	R_1 = 0.0269, wR_2 = 0.0625
Final R indexes [all data]	R_1 = 0.0400, wR_2 = 0.0676
Largest diff. peak/hole / e Å^{-3}	1.23/-0.68

Table S8. Bond Lengths for tpy2Pt.

Atom	Atom	Length/Å	Atom	Atom	Length/Å
Pt1	Cl1	2.3014(15)	C10	C16	1.471(8)
Pt1	N2	1.944(5)	C10	C11	1.370(8)
Pt1	N1	2.007(5)	N4	C14	1.319(8)
Pt1	N3	2.015(5)	N4	C13	1.321(8)
Pt3	S1	2.2055(17)	C19	C18	1.373(10)
Pt3	Cl4	2.3065(17)	C16	C17	1.386(9)
Pt3	Cl3	2.3200(17)	C8	C7	1.409(9)
Pt3	Cl2	2.3013(17)	C6	C5	1.403(9)
S1	O1	1.457(5)	C6	C1	1.403(9)
S1	C21	1.770(7)	C6	C7	1.478(8)
S1	C20	1.757(8)	C2	C3	1.391(10)
N2	C9	1.339(8)	C2	C1	1.372(9)
N2	C10	1.355(8)	C23	C24	1.494(10)
N1	C12	1.375(8)	C23	C22	1.482(10)
N1	C15	1.350(8)	C17	N5	1.325(8)
O2	C23	1.202(8)	C5	C4	1.368(9)
N3	C19	1.350(8)	C3	C4	1.364(10)
N3	C16	1.364(8)	C14	C15	1.371(9)
C12	C9	1.475(8)	C18	N5	1.338(9)
C12	C13	1.373(9)	C11	C7	1.399(9)
C9	C8	1.378(8)			

Table S9. Bond Angles for tpy2Pt.

Atom	Atom	Atom	Angle/°	Atom	Atom	Atom	Angle/°
N2	Pt1	Cl1	177.96(15)	C8	C9	C12	127.8(6)
N2	Pt1	N1	81.0(2)	N2	C10	C16	111.9(5)

N2	Pt1	N3	80.7(2)	N2	C10	C11	118.2(6)
N1	Pt1	Cl1	98.27(15)	C11	C10	C16	129.9(6)
N1	Pt1	N3	161.6(2)	C14	N4	C13	117.0(6)
N3	Pt1	Cl1	100.03(15)	N3	C19	C18	119.5(6)
S1	Pt3	Cl4	87.72(6)	N3	C16	C10	115.5(5)
S1	Pt3	Cl3	176.71(6)	N3	C16	C17	119.3(6)
S1	Pt3	Cl2	93.92(7)	C17	C16	C10	125.2(6)
Cl4	Pt3	Cl3	89.02(6)	C9	C8	C7	119.8(6)
Cl2	Pt3	Cl4	177.97(6)	C5	C6	C1	117.1(6)
Cl2	Pt3	Cl3	89.35(6)	C5	C6	C7	121.4(6)
O1	S1	Pt3	116.4(2)	C1	C6	C7	121.5(6)
O1	S1	C21	109.2(3)	C1	C2	C3	120.0(7)
O1	S1	C20	107.1(4)	O2	C23	C24	120.6(7)
C21	S1	Pt3	108.3(3)	O2	C23	C22	121.8(7)
C20	S1	Pt3	114.7(3)	C22	C23	C24	117.7(7)
C20	S1	C21	99.7(4)	N5	C17	C16	122.8(6)
C9	N2	Pt1	118.2(4)	C4	C5	C6	120.6(7)
C9	N2	C10	123.4(5)	C4	C3	C2	119.0(6)
C10	N2	Pt1	118.4(4)	N4	C14	C15	123.5(6)
C12	N1	Pt1	113.3(4)	C2	C1	C6	121.5(6)
C15	N1	Pt1	129.4(4)	N5	C18	C19	123.3(7)
C15	N1	C12	117.2(5)	C17	N5	C18	116.6(6)
C19	N3	Pt1	128.0(4)	C10	C11	C7	121.4(6)
C19	N3	C16	118.5(5)	C8	C7	C6	121.4(6)
C16	N3	Pt1	113.6(4)	C11	C7	C8	117.5(6)
N1	C12	C9	114.7(5)	C11	C7	C6	121.1(6)
C13	C12	N1	119.8(6)	N4	C13	C12	122.5(6)
C13	C12	C9	125.4(6)	N1	C15	C14	119.7(6)
N2	C9	C12	112.6(5)	C3	C4	C5	121.8(7)
N2	C9	C8	119.6(6)				

Table S10. Crystal data and structure refinement for tpy3Pt.

Empirical formula	$C_{23}H_{19}Br_2Cl_4N_3OPt_2S$
Formula weight	1077.27
Temperature/K	150.0
Crystal system	triclinic
Space group	P-1
a/Å	7.5483(7)
b/Å	12.8386(10)
c/Å	14.7671(13)
α/°	79.304(3)
β/°	75.497(3)
γ/°	83.119(3)
Volume/Å^3	1357.3(2)

Z	2
ρ_{calc}mg/mm^3	2.636
m/mm^{-1}	13.734
F(000)	992.0
Crystal size/mm^3	0.20 × 0.18 × 0.17
2Θ range for data collection	4.674 to 50.018°
Index ranges	$-8 \le h \le 8$, $-15 \le k \le 15$, $-17 \le l \le 17$
Reflections collected	29274
Independent reflections	4768[R(int) = 0.0639]
Data/restraints/parameters	4768/0/292
Goodness-of-fit on F^2	1.217
Final R indexes [I>=2σ (I)]	R_1 = 0.0903, wR_2 = 0.2135
Final R indexes [all data]	R_1 = 0.0988, wR_2 = 0.2202
Largest diff. peak/hole / e Å^{-3}	2.91/-5.17

Table S11. Bond Lengths for tpy3Pt.

Atom	Atom	Length/Å	Atom	Atom	Length/Å
Pt2	S1	2.198(5)	C7	C11	1.3900
Pt2	Cl3	2.325(5)	C7	C6	1.512(12)
Pt2	Cl4	2.319(5)	C11	C10	1.3900
Pt2	Cl2	2.296(5)	C10	C17	1.49(2)
Pt1	Cl1	2.294(6)	N2	C16	1.3900
Pt1	N3	2.034(19)	N2	C12	1.3900
Pt1	N1	1.866(8)	C16	C15	1.3900
Pt1	N2	1.995(9)	C15	C14	1.3900
Br1	C2	1.887(10)	C14	C13	1.3900
Br2	C4	1.852(10)	C13	C12	1.3900
S1	O1	1.452(17)	C21	C20	1.36(3)
S1	C22	1.74(3)	C17	C18	1.34(3)
S1	C23	1.77(2)	C1	C6	1.3900
N3	C21	1.32(3)	C1	C2	1.3900
N3	C17	1.36(3)	C6	C5	1.3900
N1	C9	1.3900	C5	C4	1.3900
N1	C10	1.3900	C4	C3	1.3900
C9	C8	1.3900	C3	C2	1.3900
C9	C12	1.434(12)	C18	C19	1.37(3)
C8	C7	1.3900	C19	C20	1.43(3)

Table S12. Bond Angles for tpy3Pt.

Atom	Atom	Atom	Angle/°	Atom	Atom	Atom	Angle/°
S1	Pt2	Cl3	176.7(2)	N1	C10	C17	109.5(11)
S1	Pt2	Cl4	86.7(2)	C11	C10	N1	120.0

S1	Pt2	Cl2	93.1(2)	C11	C10	C17	130.5(11)
Cl4	Pt2	Cl3	90.74(19)	C16	N2	Pt1	126.5(7)
Cl2	Pt2	Cl3	89.5(2)	C16	N2	C12	120.0
Cl2	Pt2	Cl4	178.0(2)	C12	N2	Pt1	113.4(7)
N3	Pt1	Cl1	98.4(6)	C15	C16	N2	120.0
N1	Pt1	Cl1	179.0(4)	C16	C15	C14	120.0
N1	Pt1	N3	80.7(6)	C13	C14	C15	120.0
N1	Pt1	N2	81.6(5)	C14	C13	C12	120.0
N2	Pt1	Cl1	99.4(4)	N2	C12	C9	113.8(9)
N2	Pt1	N3	162.2(6)	C13	C12	C9	126.2(9)
O1	S1	Pt2	115.7(7)	C13	C12	N2	120.0
O1	S1	C22	106.9(12)	N3	C21	C20	124(2)
O1	S1	C23	107.3(12)	N3	C17	C10	115.0(17)
C22	S1	Pt2	113.7(9)	C18	C17	N3	122(2)
C22	S1	C23	102.1(13)	C18	C17	C10	122.7(18)
C23	S1	Pt2	110.1(9)	C6	C1	C2	120.0
C21	N3	Pt1	128.6(16)	C1	C6	C7	119.8(10)
C21	N3	C17	117.8(19)	C5	C6	C7	120.1(10)
C17	N3	Pt1	113.5(14)	C5	C6	C1	120.0
C9	N1	Pt1	118.7(6)	C6	C5	C4	120.0
C9	N1	C10	120.0	C5	C4	Br2	122.1(8)
C10	N1	Pt1	121.3(6)	C3	C4	Br2	117.9(8)
N1	C9	C8	120.0	C3	C4	C5	120.0
N1	C9	C12	112.4(9)	C4	C3	C2	120.0
C8	C9	C12	127.6(9)	C1	C2	Br1	122.0(8)
C7	C8	C9	120.0	C3	C2	Br1	117.9(8)
C8	C7	C6	120.6(9)	C3	C2	C1	120.0
C11	C7	C8	120.0	C17	C18	C19	121(2)
C11	C7	C6	119.4(9)	C18	C19	C20	117(2)
C7	C11	C10	120.0	C21	C20	C19	118(2)

Table S13. Crystal data and structure refinement for tpy4Pt.

Empirical formula	$C_{16}H_{15}Cl_2N_3O_2Pt$
Formula weight	547.30
Temperature/K	150.0
Crystal system	triclinic
Space group	P-1
a/Å	7.4848(7)
b/Å	8.8709(8)
c/Å	13.4498(12)
α/°	73.384(3)
β/°	76.458(3)

γ/°	73.499(3)
Volume/Å^3	809.05(13)
Z	2
ρ_{calc}mg/mm^3	2.247
m/mm^{-1}	9.016
F(000)	520.0
Crystal size/mm^3	0.35 × 0.33 × 0.31
2Θ range for data collection	4.928 to 50.018°
Index ranges	-8 ≤ h ≤ 8, -10 ≤ k ≤ 10, -16 ≤ l ≤ 16
Reflections collected	17161
Independent reflections	2847[R(int) = 0.0829]
Data/restraints/parameters	2847/0/219
Goodness-of-fit on F^2	1.000
Final R indexes [I>=2σ (I)]	R_1 = 0.0542, wR_2 = 0.1377
Final R indexes [all data]	R_1 = 0.0608, wR_2 = 0.1425
Largest diff. peak/hole / e Å^{-3}	3.40/-3.26

Table S14. Bond Lengths for tpy4Pt.

Atom	Atom	Length/Å	Atom	Atom	Length/Å
Pt1	Cl1	2.303(3)	C6	C7	1.391(16)
Pt1	N2	1.903(10)	C10	C9	1.400(17)
Pt1	N1	2.051(11)	C10	C11	1.468(19)
Pt1	N3	2.034(11)	C5	C4	1.379(18)
N2	C6	1.356(18)	C15	C14	1.379(19)
N2	C10	1.349(17)	C1	C2	1.36(2)
O1	C8	1.354(15)	C2	C3	1.36(2)
O2	C16	1.49(2)	C8	C7	1.377(18)
N1	C5	1.374(16)	C8	C9	1.409(17)
N1	C1	1.296(17)	C12	C11	1.362(18)
N3	C15	1.349(16)	C12	C13	1.373(19)
N3	C11	1.352(17)	C4	C3	1.382(19)
C6	C5	1.436(18)	C14	C13	1.41(2)

Table S15. Bond Angles for tpy4Pt.

Atom	Atom	Atom	Angle/°	Atom	Atom	Atom	Angle/°
N2	Pt1	Cl1	179.3(4)	C9	C10	C11	126.9(12)
N2	Pt1	N1	81.4(5)	N1	C5	C6	116.8(11)
N2	Pt1	N3	80.8(5)	N1	C5	C4	117.8(11)
N1	Pt1	Cl1	97.9(3)	C4	C5	C6	125.4(12)
N3	Pt1	Cl1	99.9(3)	N3	C15	C14	118.8(13)

N3	Pt1	N1	162.1(4)	N1	C1	C2	120.9(13)
C6	N2	Pt1	118.5(9)	C3	C2	C1	120.0(13)
C10	N2	Pt1	118.7(9)	O1	C8	C7	116.9(10)
C10	N2	C6	122.9(11)	O1	C8	C9	122.0(12)
C5	N1	Pt1	110.5(9)	C7	C8	C9	121.0(11)
C1	N1	Pt1	127.3(9)	C8	C7	C6	119.4(12)
C1	N1	C5	122.3(12)	C11	C12	C13	119.9(13)
C15	N3	Pt1	125.2(10)	C5	C4	C3	120.0(12)
C15	N3	C11	121.6(12)	C10	C9	C8	117.4(12)
C11	N3	Pt1	113.2(8)	N3	C11	C10	114.4(11)
N2	C6	C5	112.8(10)	N3	C11	C12	121.0(12)
N2	C6	C7	119.1(12)	C12	C11	C10	124.6(12)
C7	C6	C5	128.2(12)	C15	C14	C13	120.3(13)
N2	C10	C9	120.1(12)	C12	C13	C14	118.4(12)
N2	C10	C11	112.9(11)	C2	C3	C4	119.0(13)

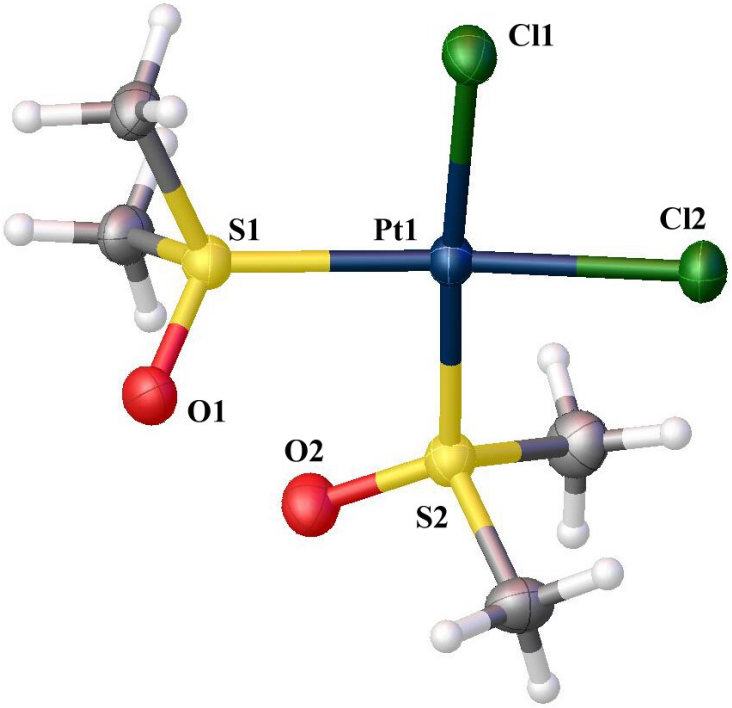

Figure S1. ORTEP view of **PtS**.

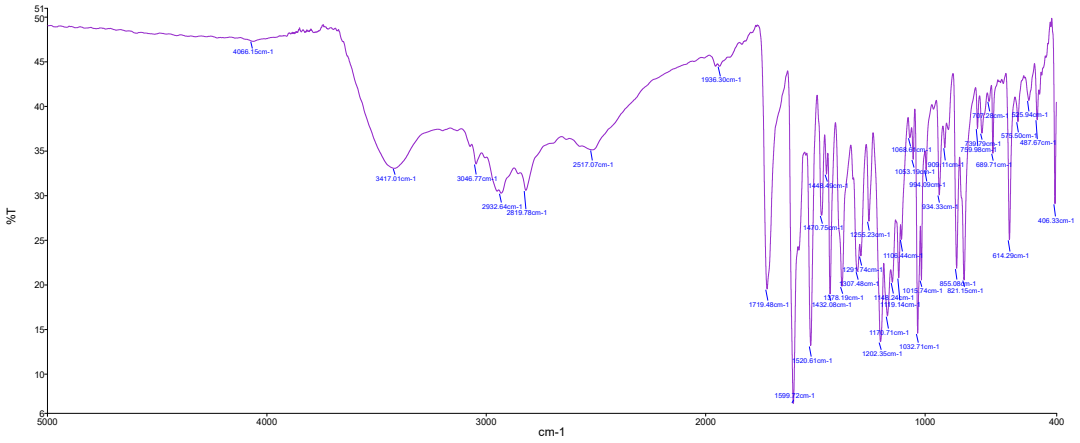

Figure S2. IR (KBr) spectra of tpy1.

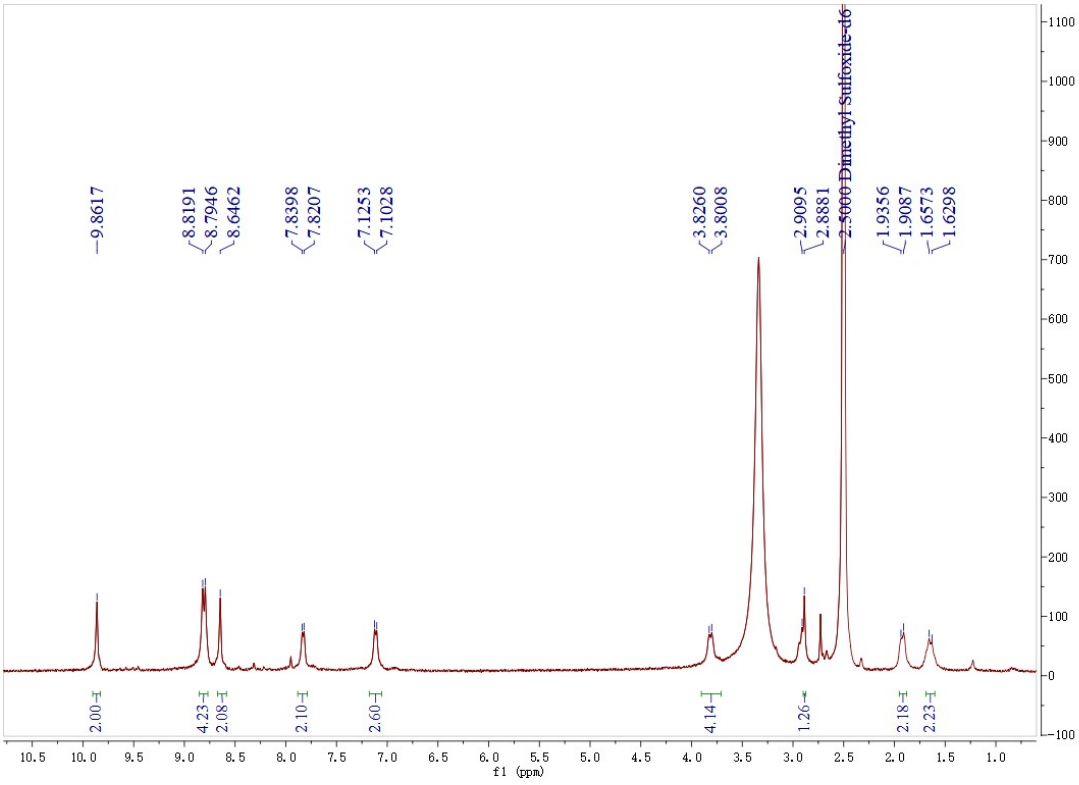

Figure S3. ^{1}H NMR (400MHz, DMSO-d6) for complex tpy1.

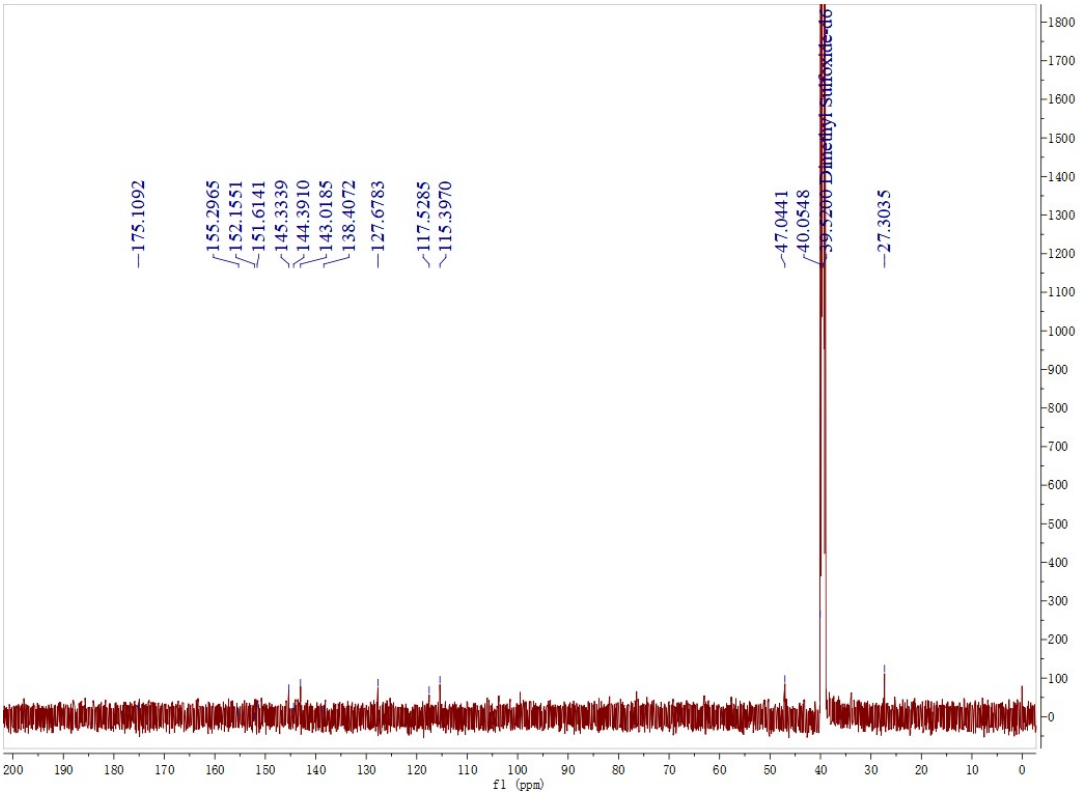

Figure S4. ^{13}C NMR (101MHz, DMSO-d6) for complex tpy1.

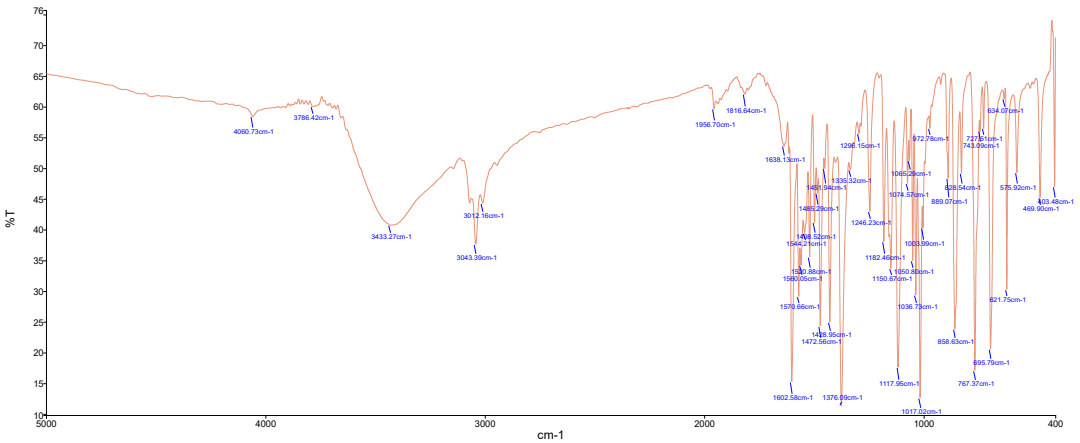

Figure S5. IR (KBr) spectra of tpy2.

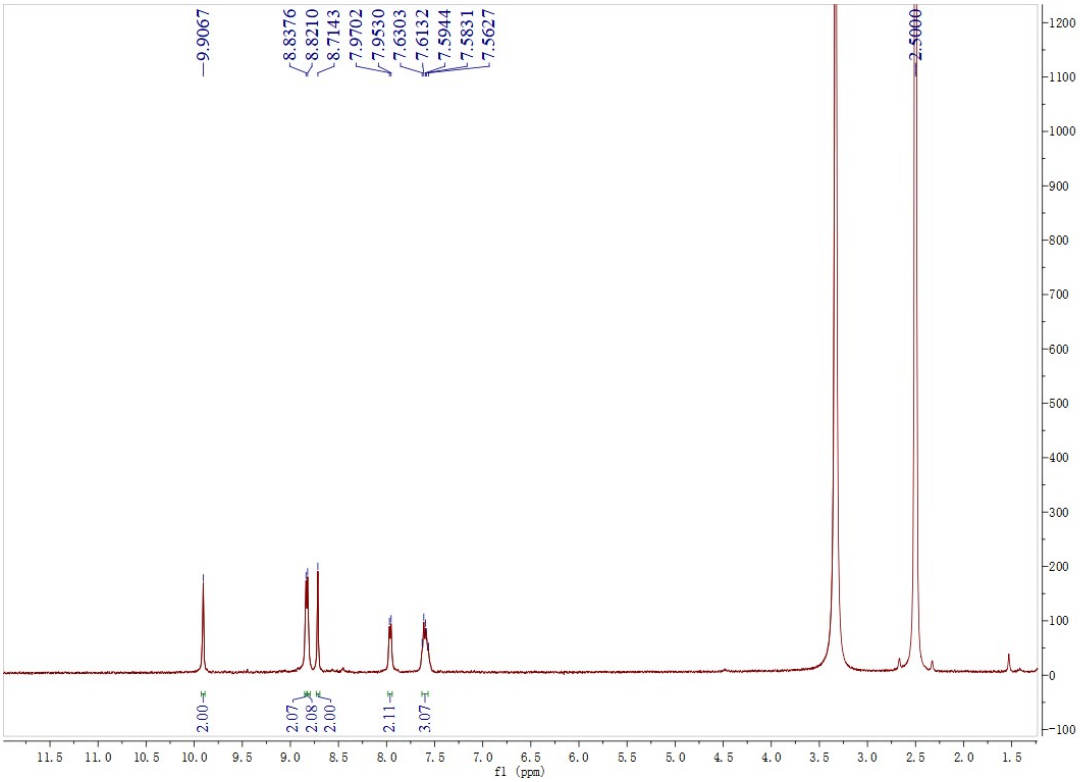

Figure S6. ^{1}H NMR (400MHz, DMSO-d6) for complex tpy2.

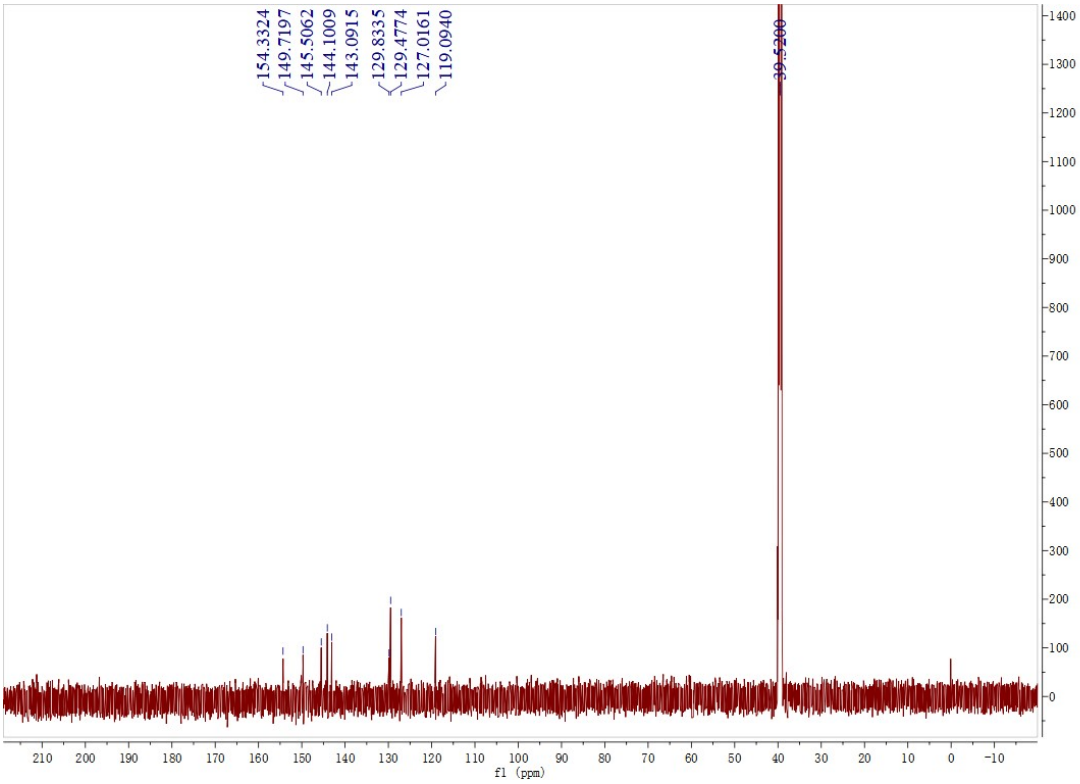

Figure S7. ^{13}C NMR (101MHz, DMSO-d6) for complex tpy2.

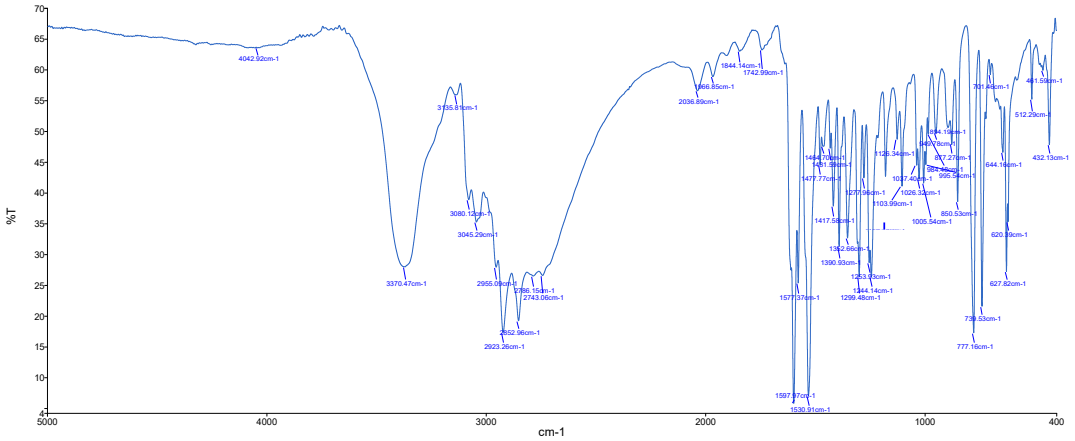

Figure S8. IR (KBr) spectra of tpy3.

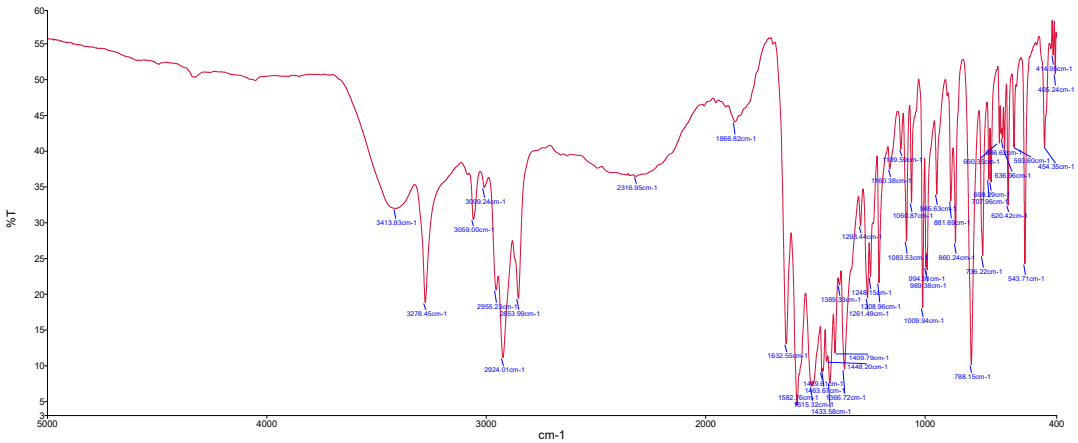

Figure S9. IR (KBr) spectra of tpy4.

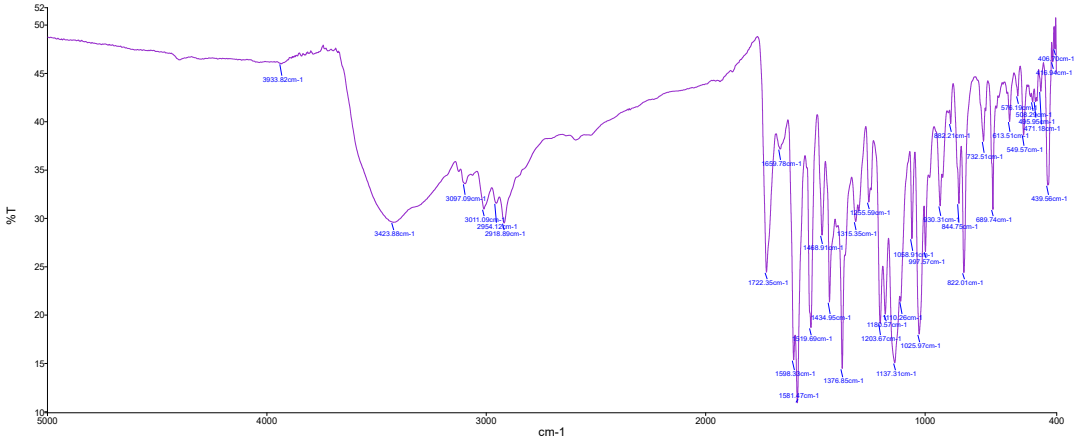

Figure S10. IR (KBr) spectra of **tpy1Pt**.

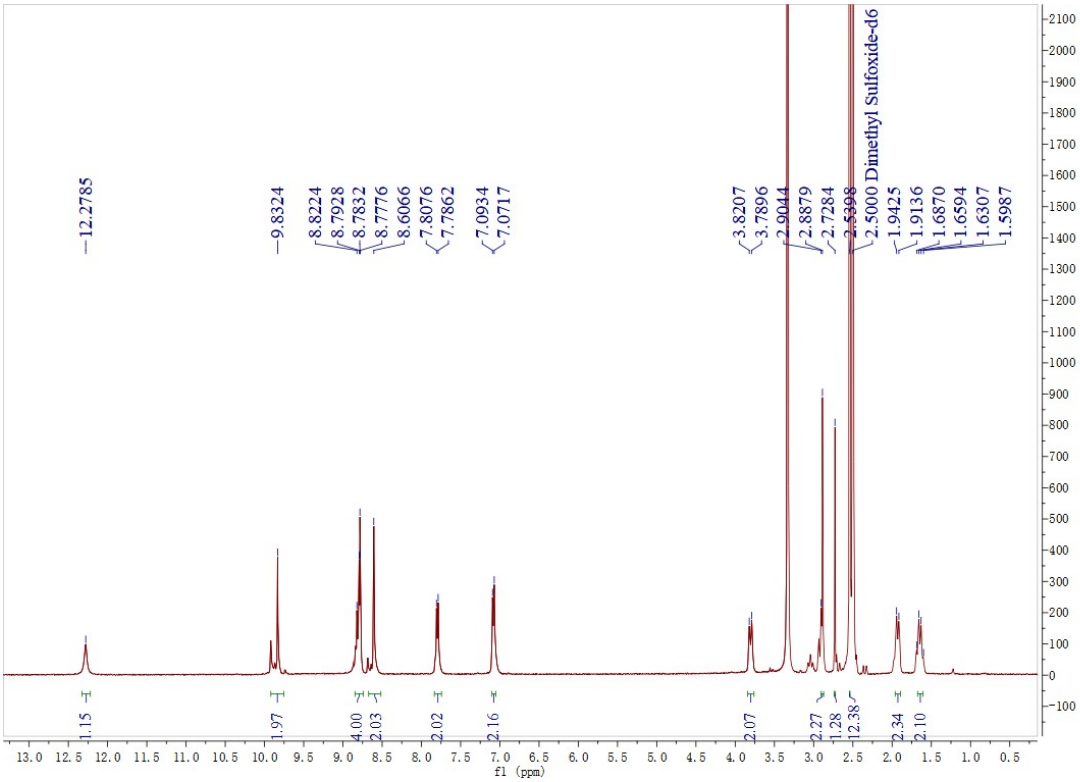

Figure S11. ^{1}H NMR (500MHz, DMSO-d6) for complex **tpy1Pt**.

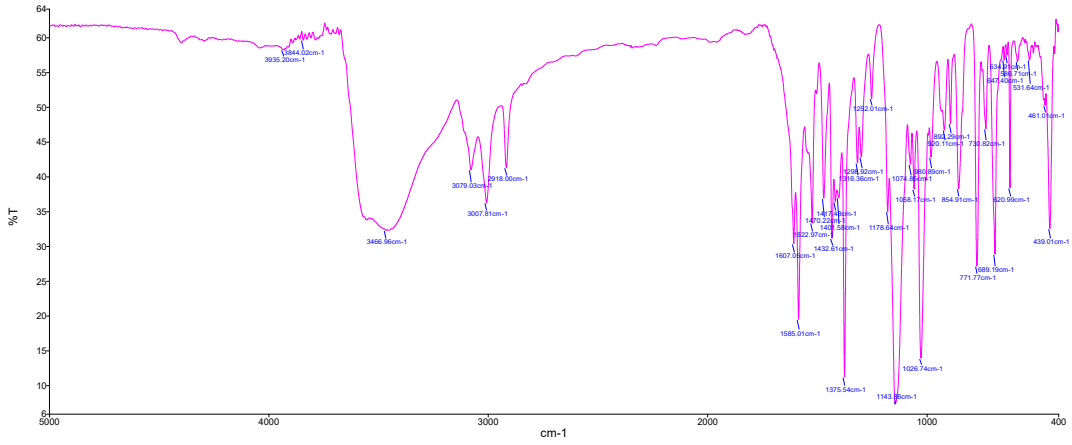

Figure S12. IR (KBr) spectra of **tpy2Pt**.

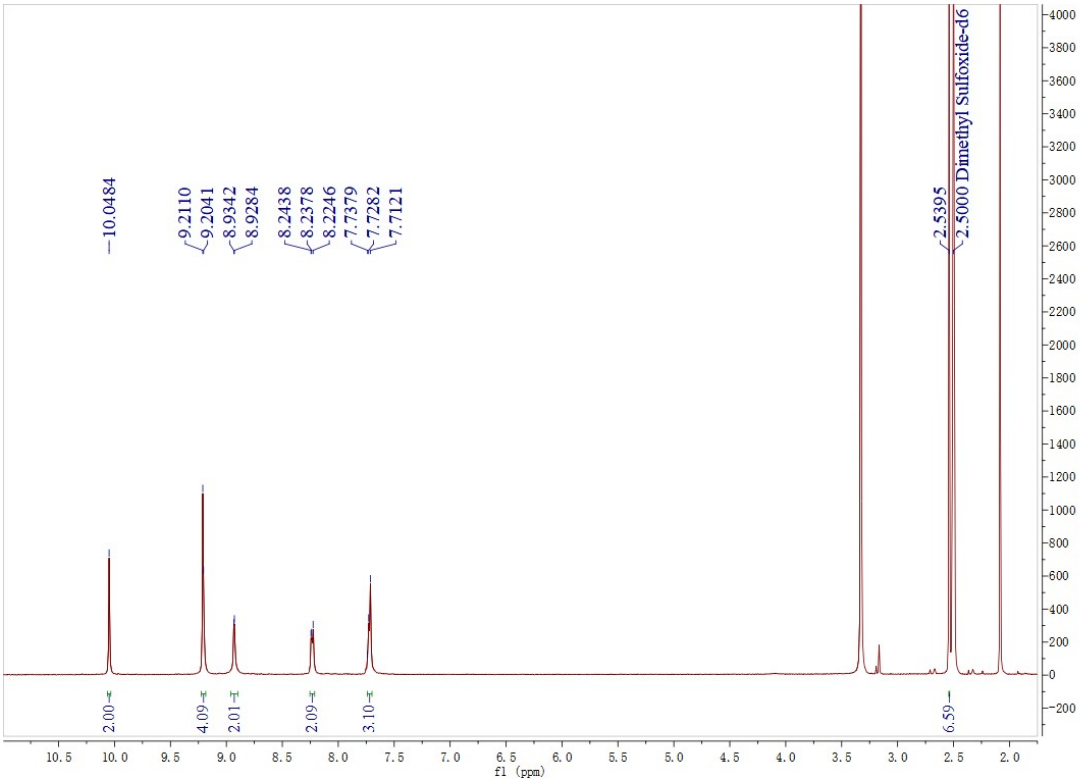

Figure S13. ^{1}H NMR (500MHz, DMSO-d6) for complex **tpy2Pt**.

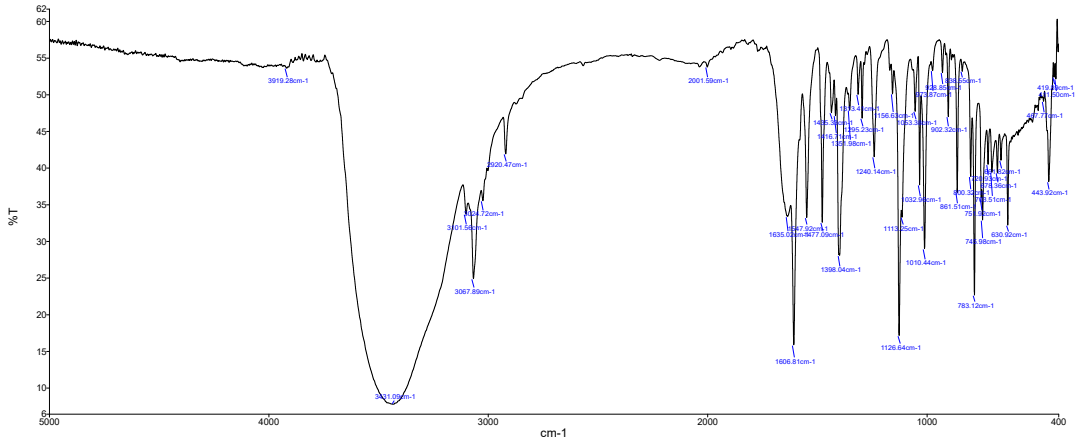

Figure S14. IR (KBr) spectra of **tpy3Pt**.

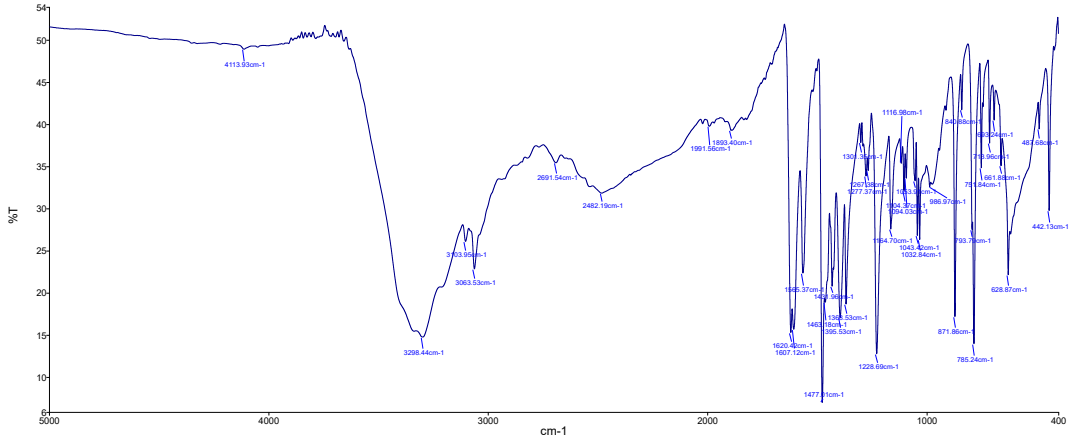

Figure S15. IR (KBr) spectra of **tpy4Pt**.

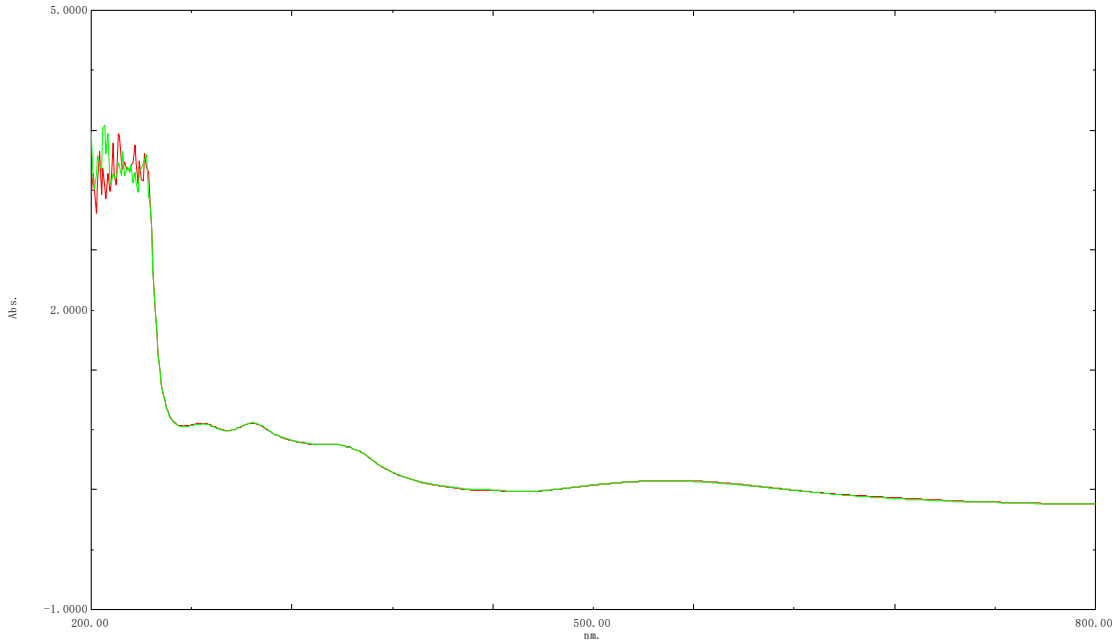

Figure S16. UV-Vis absorption spectra of **tpy1Pt** (5.0×10^{-5} M) in Tris-HCl solution in the time course 0 h and 48 h, respectively.

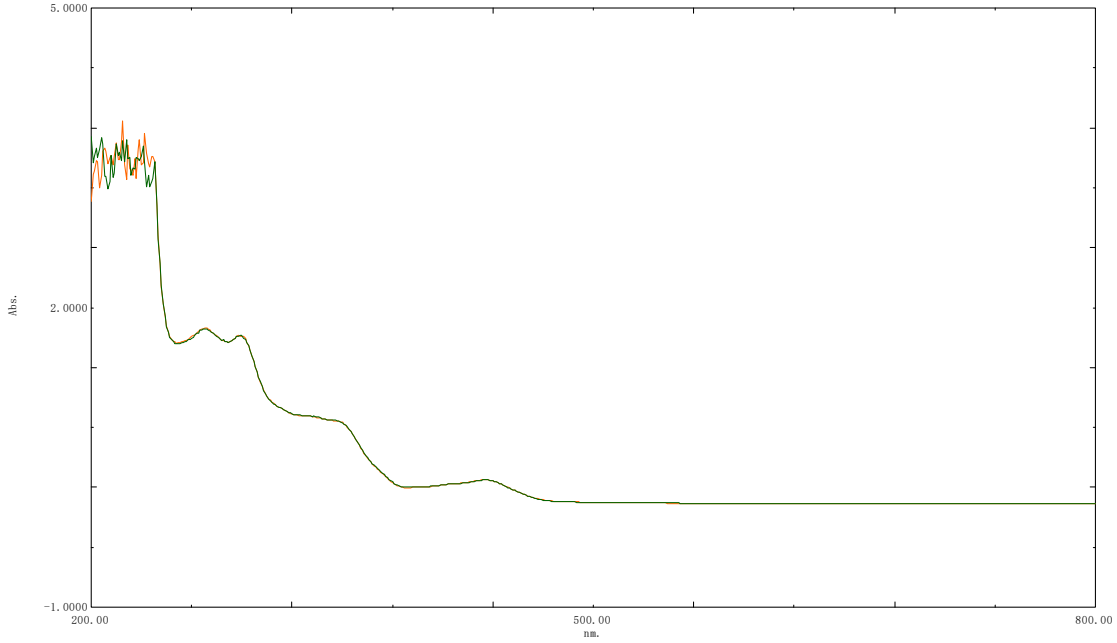

Figure S17. UV-Vis absorption spectra of **tpy2Pt** (5.0×10^{-5} M) in Tris-HCl solution in the time course 0 h and 48 h, respectively.

Table S16. The tumor volume (cm^3) in **tpy1Pt** treated and non-treated mice from the date of surgery to the study end point in the SK-OV-3 xenograft model (mean±SD, n=6).

	1day	3day	5day	7day	9day	11day	13day	15day	17day	19day	21day
control	0.102±0.006	0.142±0.014	0.217±0.034	0.364±0.049	0.531±0.055	0.698±0.041	0.818±0.038	0.95±0.039	1.074±0.049	1.188±0.046	1.404±0.091
tpy1Pt	0.097±0.01	0.1393±0.014	0.205±0.014	0.311±0.043	0.392±0.052	0.432±0.049	0.472±0.051	0.497±0.057	0.518±0.039	0.569±0.047	0.658±0.036

* p <0.05, p *vs* vehicle control.

Table S17. Average body weight (g) in **tpy1Pt** treated and non-treated mice from the date of surgery to the study end point in the SK-OV-3 xenograft model (mean±SD, n=6).

	1day	3day	5day	7day	9day	11day	13day	15day	17day	19day	21day
control	18.8±0.4	18.9±0.3	19.3±0.3	19.6±0.4	19.9±0.4	20.2±0.4	20.6±0.4	20.7±0.2	20.9±0.3	21.1±0.3	21.4±0.3
tpy1Pt	18.4±0.6	18.6±0.6	18.8±0.6	19.1±0.6	19.3±0.6	19.6±0.6	19.8±0.6	19.9±0.6	20.1±0.6	20.3±0.6	20.4±0.7

* p <0.05, p *vs* vehicle control.

Table S18. In vivo anti-cancer activity of **tpy1Pt** 5.0 mg/kg) toward SK-OV-3 tumor xenograft (mean±SD, n=6).

	mg/kg	average tumor weight (mean ± SD, g)	inhibition of tumor growth (%)
control	-	1.84±0.13	-
tpy1Pt	5.0	0.87±0.10*	52.4

* p <0.05, p *vs* vehicle control.

Table S19. The levels of 8-OHdG in SKO3cisR cells treated with **tpy1Pt** (0.23μM) and **tpy2Pt** (1.97μM), respectively.

groups	control	**Tpy2Pt**	**tpy1Pt**
OD values	0.3154	0.3698	0.4463
	0.3342	0.3549	0.4597
	0.3066	0.3863	0.4947
8-OHdG (ng/mL)	8.18	9.92	12.36
	8.78	9.44	12.79
	7.90	10.45	13.90
mean	8.29	9.94	13.02
SD	0.45	0.50	0.80

Table S20. Levels of ATP in SKO3cisR cells after treated with **tpy1Pt** (0.23μM) and **tpy2Pt** (1.97μM) for 48 h (n = 3, $p < 0.05$).

groups	control	**Tpy2Pt**	**tpy1Pt**
OD values	49915	42896	18960
	53819	45556	17872
	54871	46709	19453
correction of OD values	49894	42875	18939
	53798	45535	17851
	54850	46688	19432
ATP values (μM)	5.02	4.32	1.93
	5.41	4.59	1.82
	5.52	4.70	1.98
Mean	5.32	4.54	1.91
SD	0.26	0.20	0.08

Table S21. Levels of mitochondrial respiratory chain complex I in SKO3cisR cells after treated with **tpy1Pt** (0.23μM) and **tpy2Pt** (1.97μM) for 48 h (n = 3, p < 0.05).

groups	ΔA	Cpr	the levels of mitochondrial respiratory chain complex I (U/mg prot)	Mean	SD
control	0.0979	1.880	83.74	82.33	4.31
	0.0895	1.678	85.76		
	0.0683	1.417	77.49		
Tpy2Pt	0.069	1.625	68.27	71.16	2.55
	0.1068	2.350	73.09		
	0.0992	2.212	72.13		
tpy1Pt	0.0403	2.322	27.91	29.96	2.22
	0.028	1.518	29.66		
	0.0309	1.537	32.32		

ΔA: Measured value for each sample; Cpr: The protein concentration of each sample; All assays and calculation process were performed according to the manufacturer's instructions (mitochondrial respiratory chain complexes I and IV, Solarbio Life Sciences, Beijing, China).

Table S22. Levels of mitochondrial respiratory chain complex IV in SKO3cisR cells after treated with **tpy1Pt** (0.23μM) and **tpy2Pt** (1.97μM) for 48 h (n = 3, $p < 0.05$).

groups	ΔA	Cpr	the levels of mitochondrial respiratory chain complex IV (U/mg prot)	Mean	SD
control	0.0857	1.338	70.39	71.48	2.91
	0.0607	0.892	74.78		
	0.0863	1.369	69.27		
Tpy2Pt	0.0899	1.725	57.28	60.71	4.14
	0.0563	0.947	65.31		
	0.0807	1.489	59.55		
tpy1Pt	0.0289	1.110	28.62	29.54	2.06
	0.0253	0.872	31.90		
	0.0209	0.818	28.09		

Original images of western blotting experiments

Beclin-1

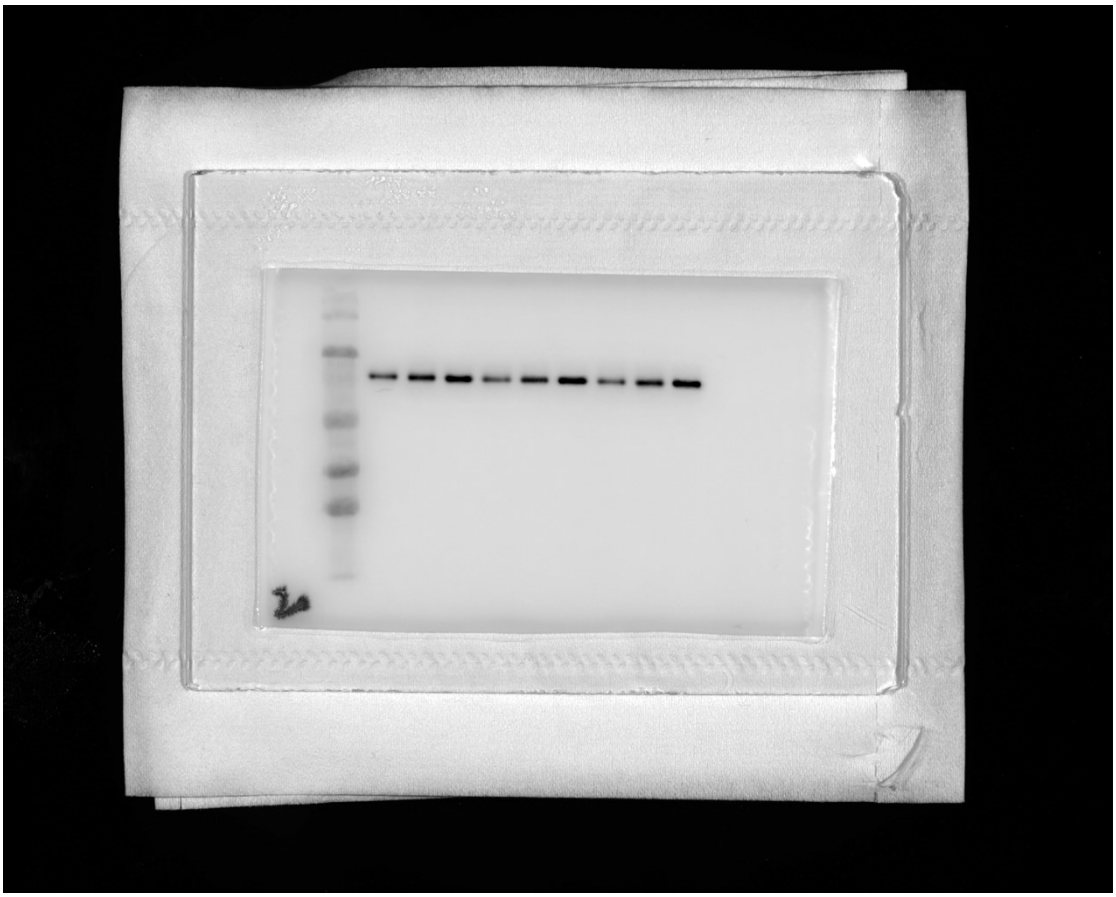

Caspase-9

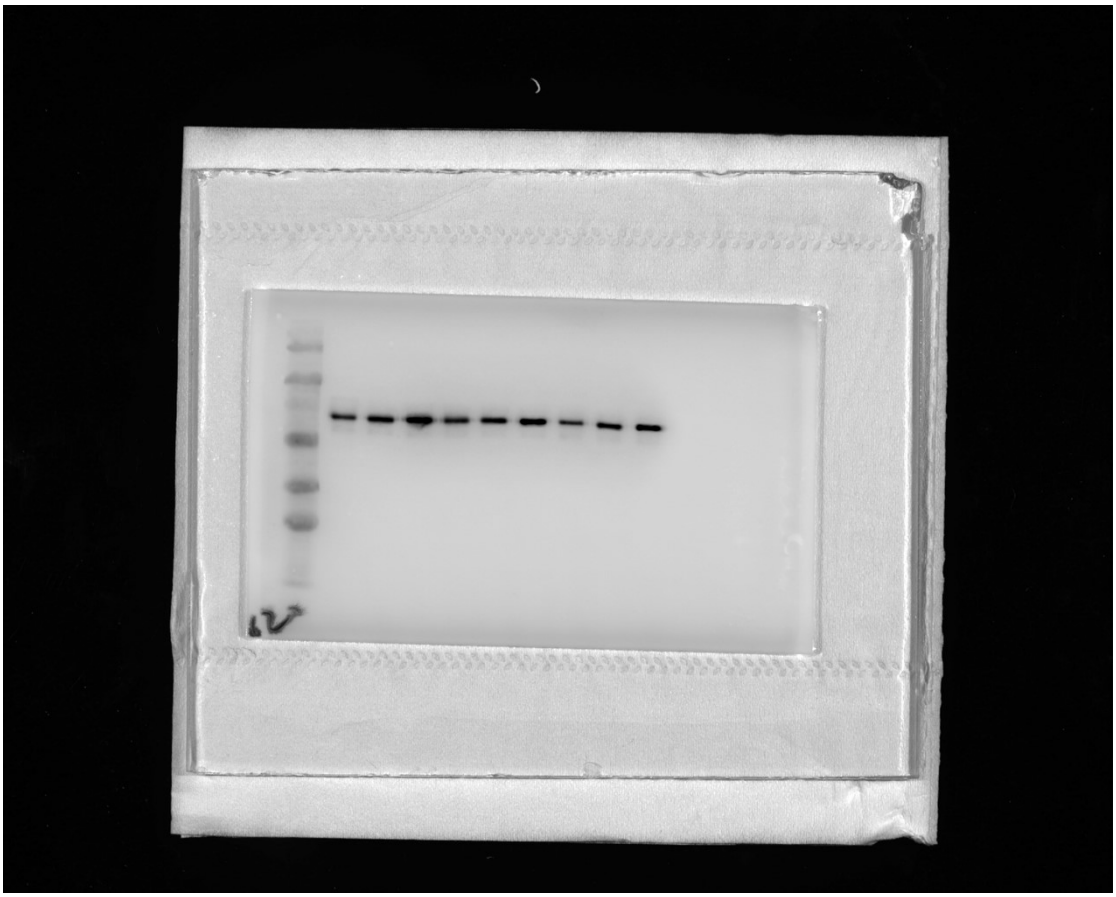

cleaved-Caspase-3

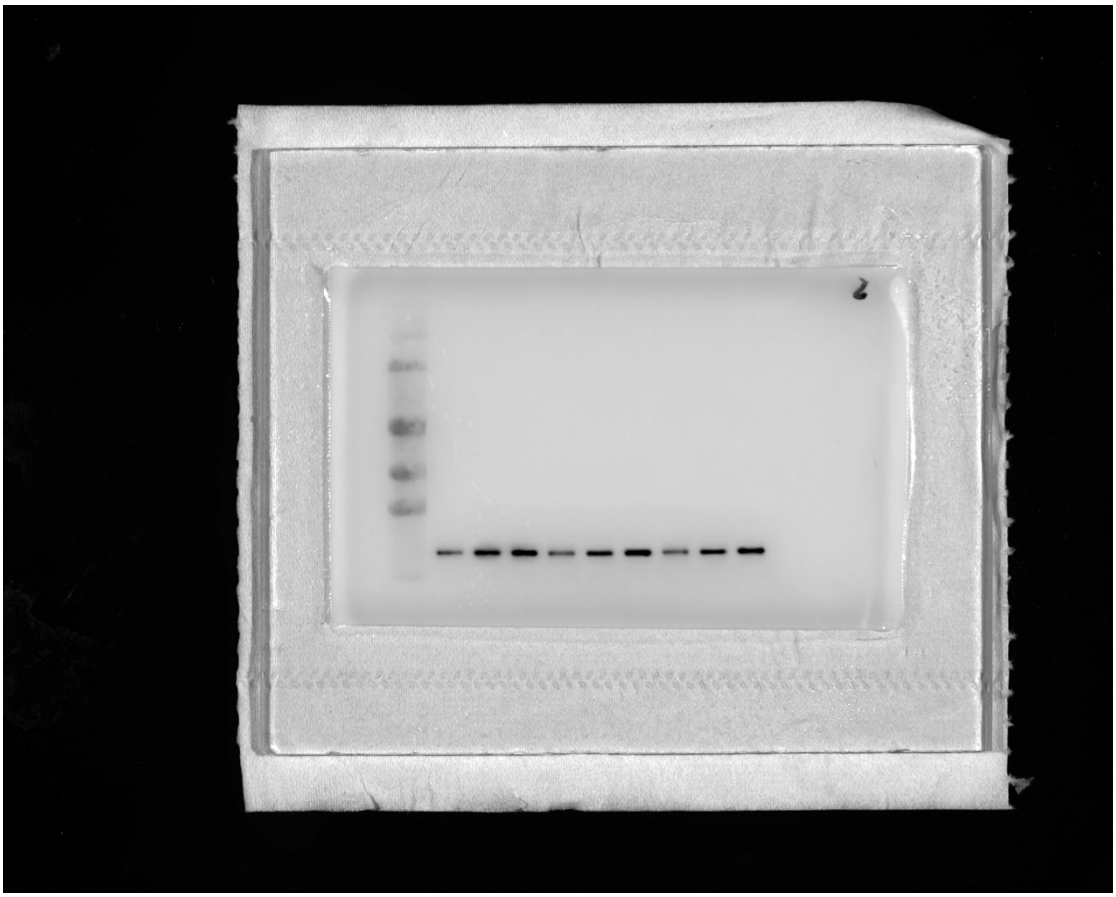

Cytochrome c

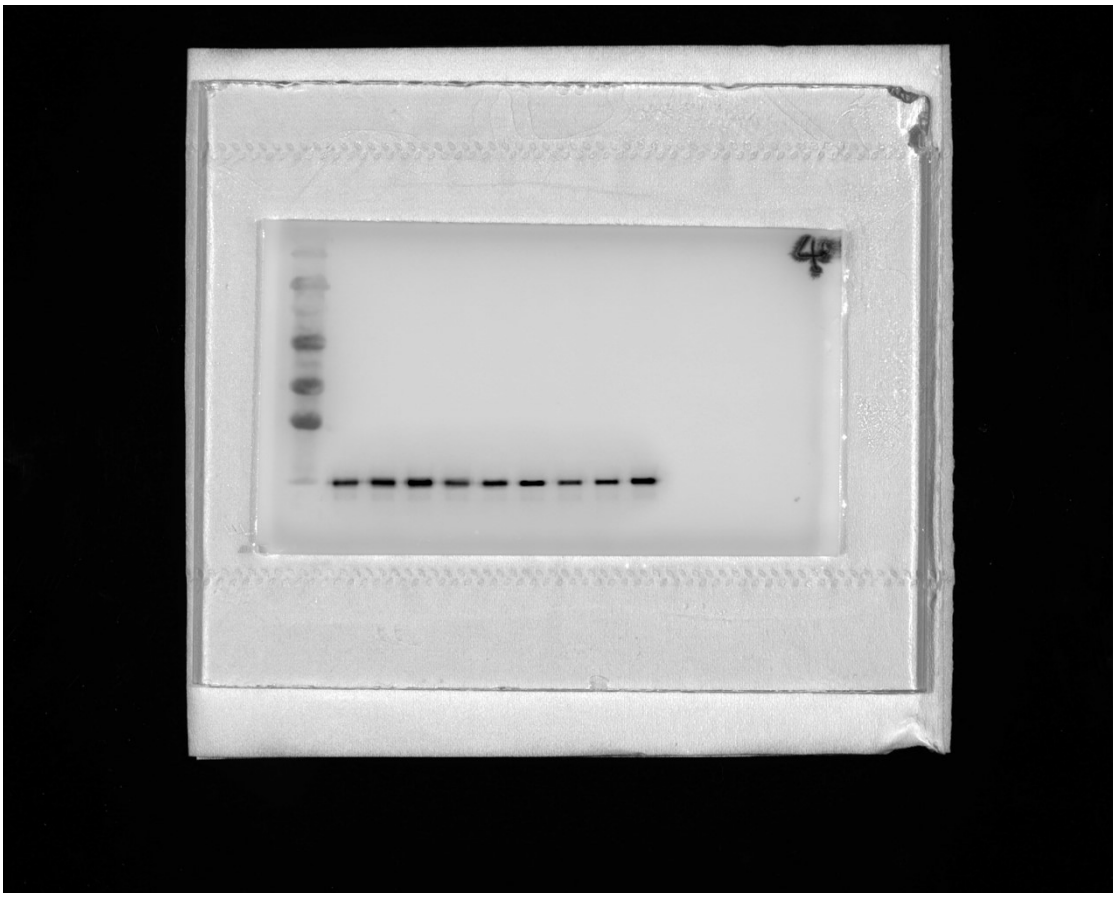

FUNDC1

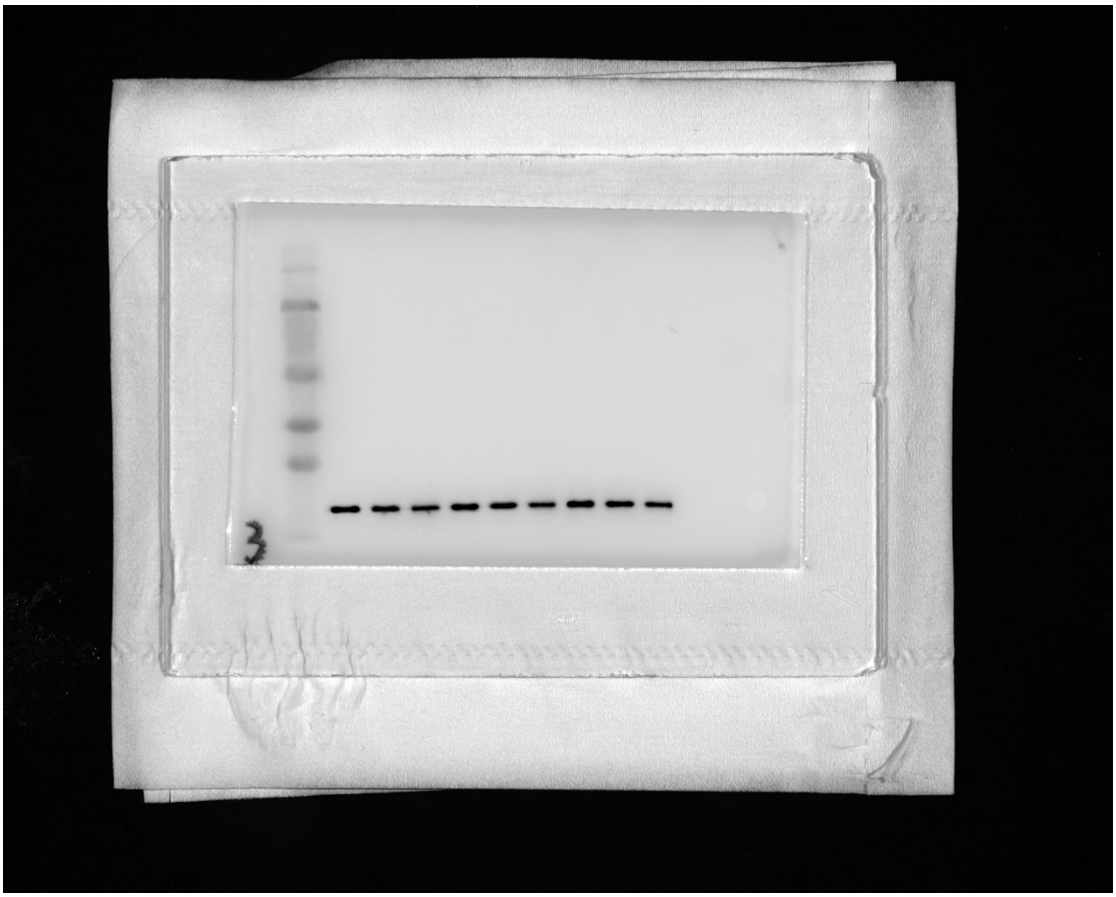

GAPDH-1

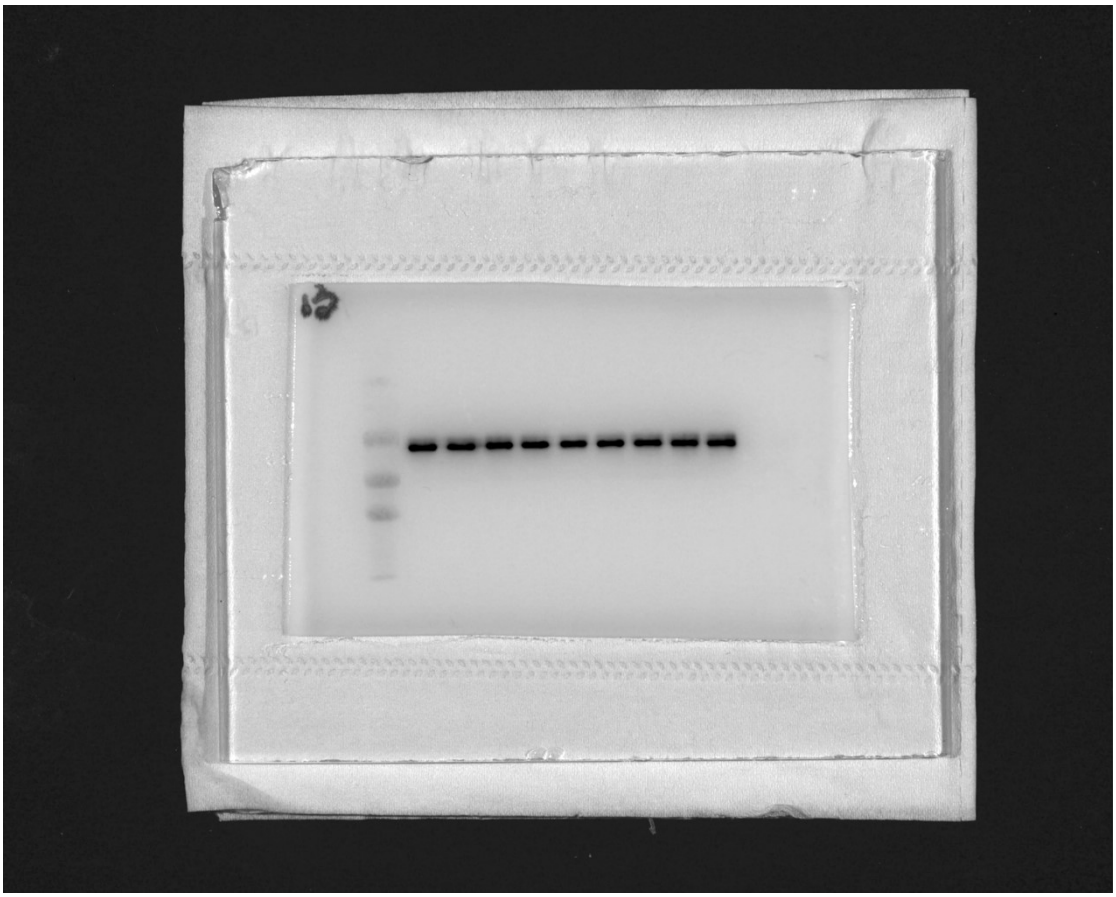

GAPDH-2

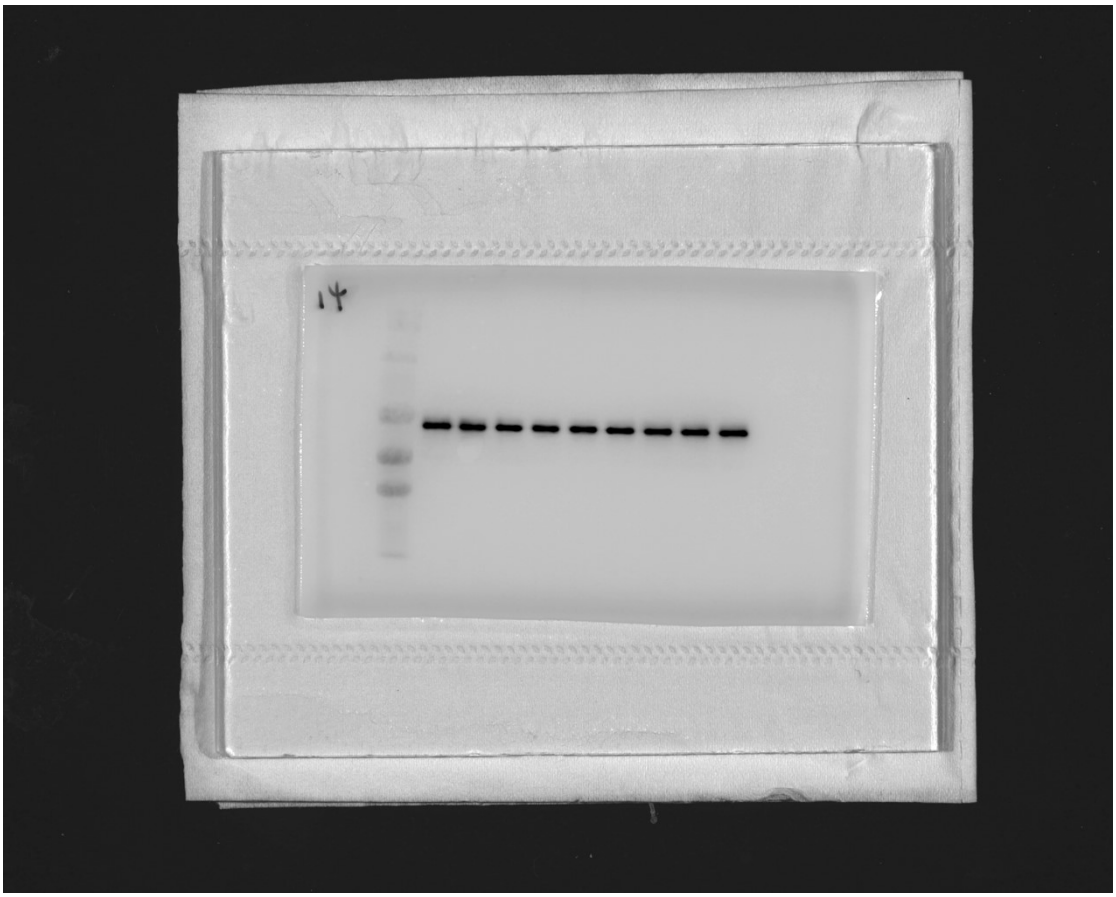

LC3

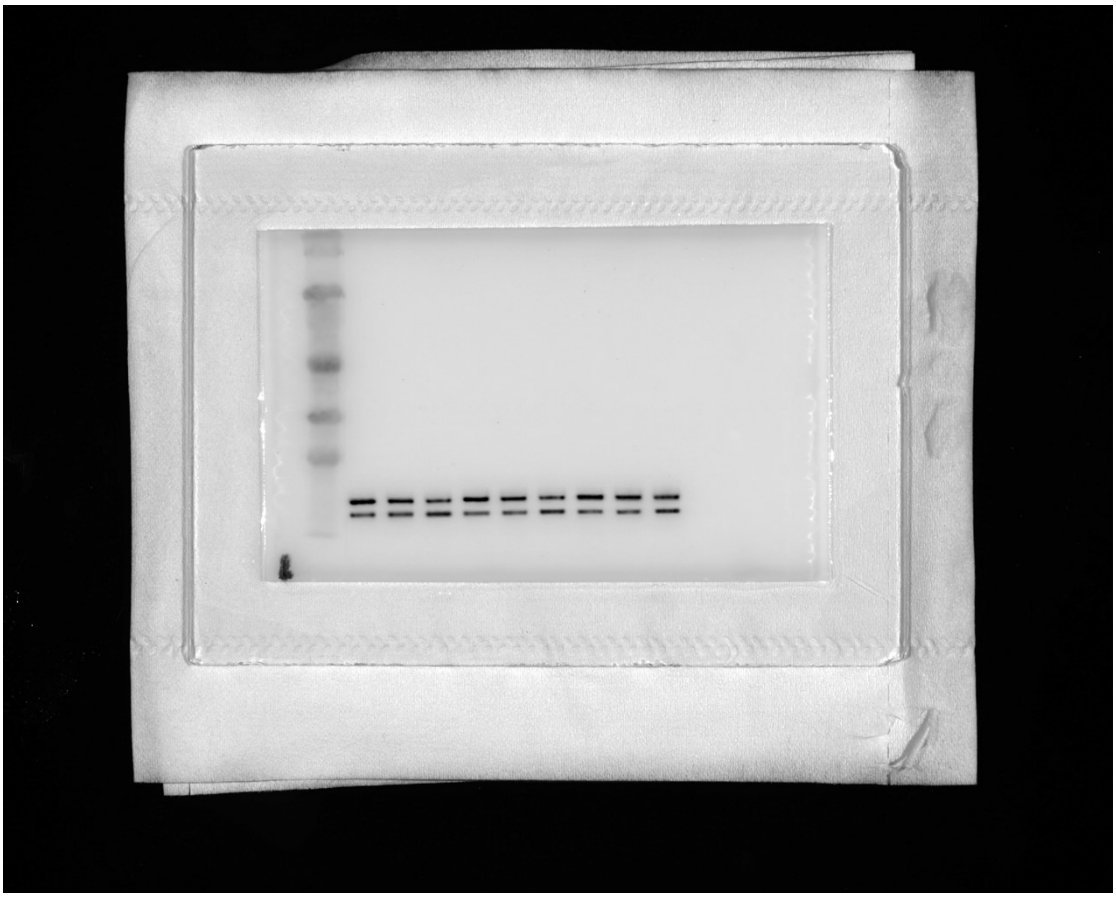

P62

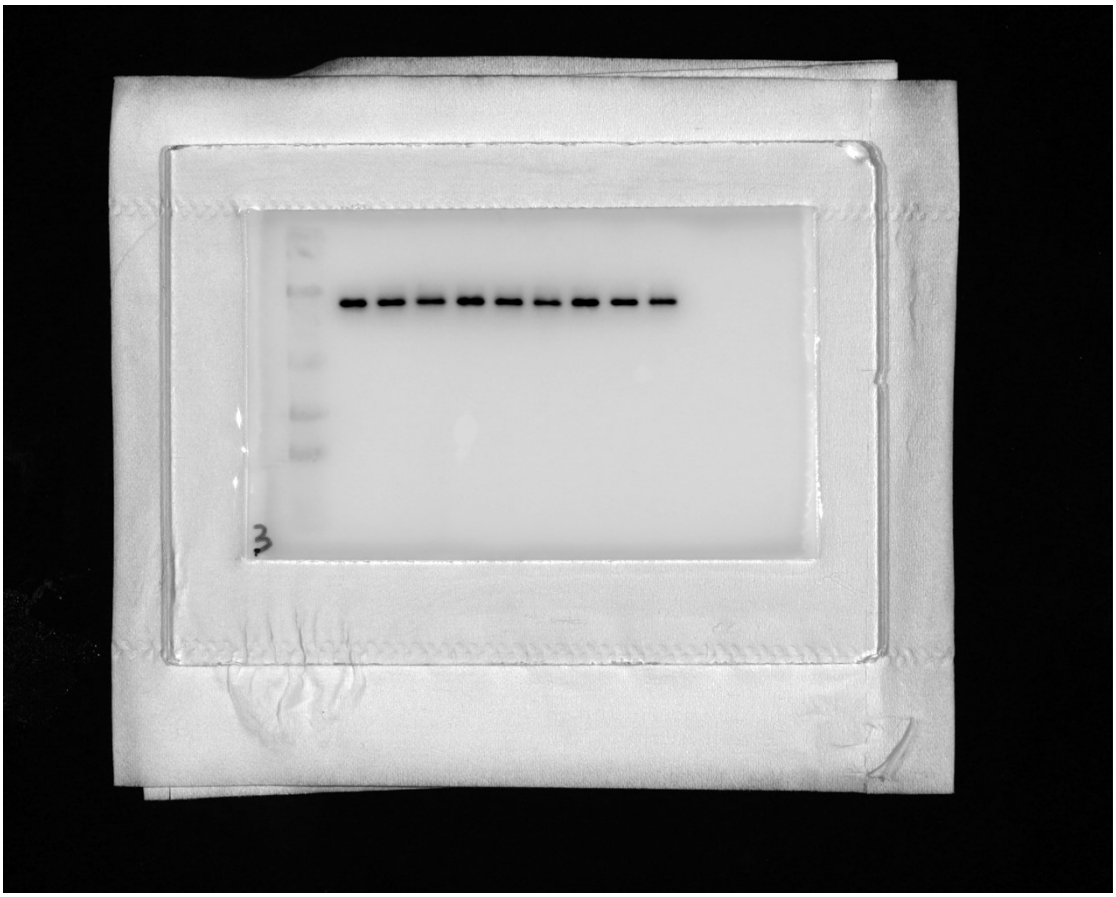

Parkin

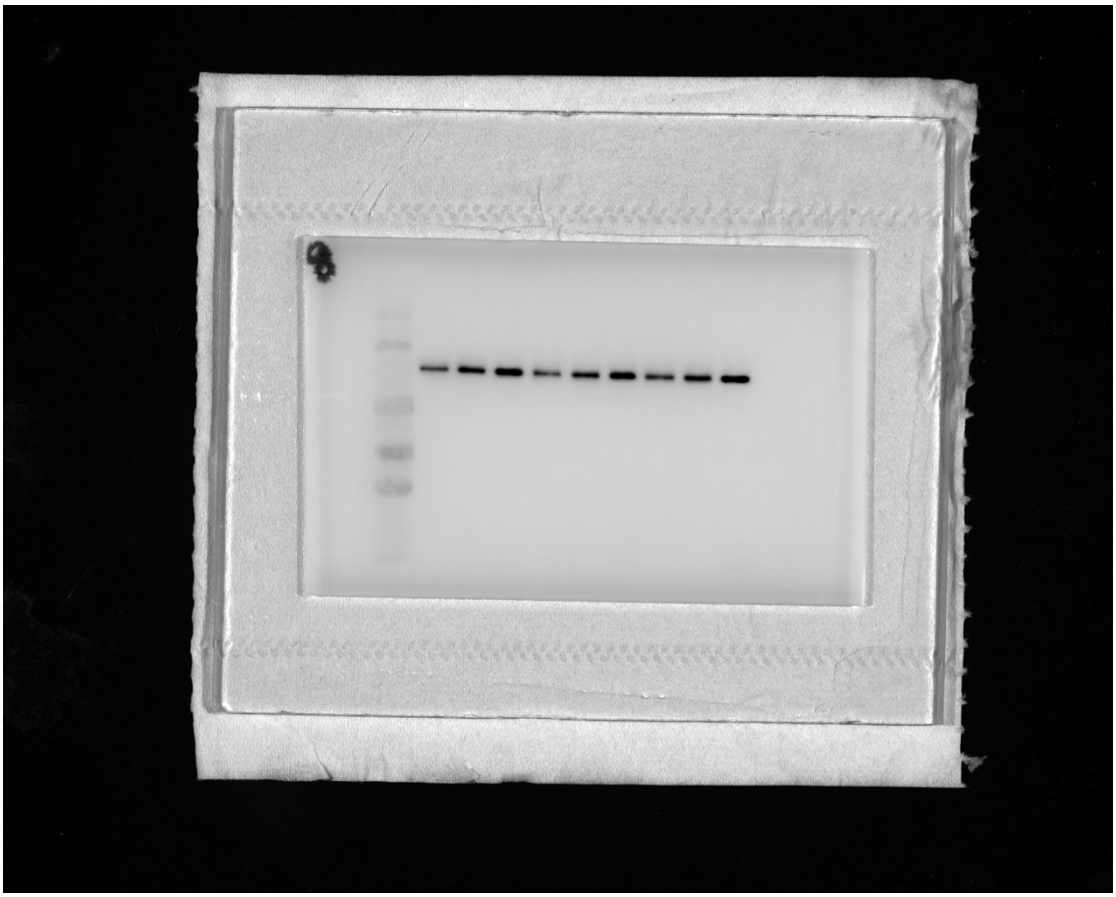

PINK1

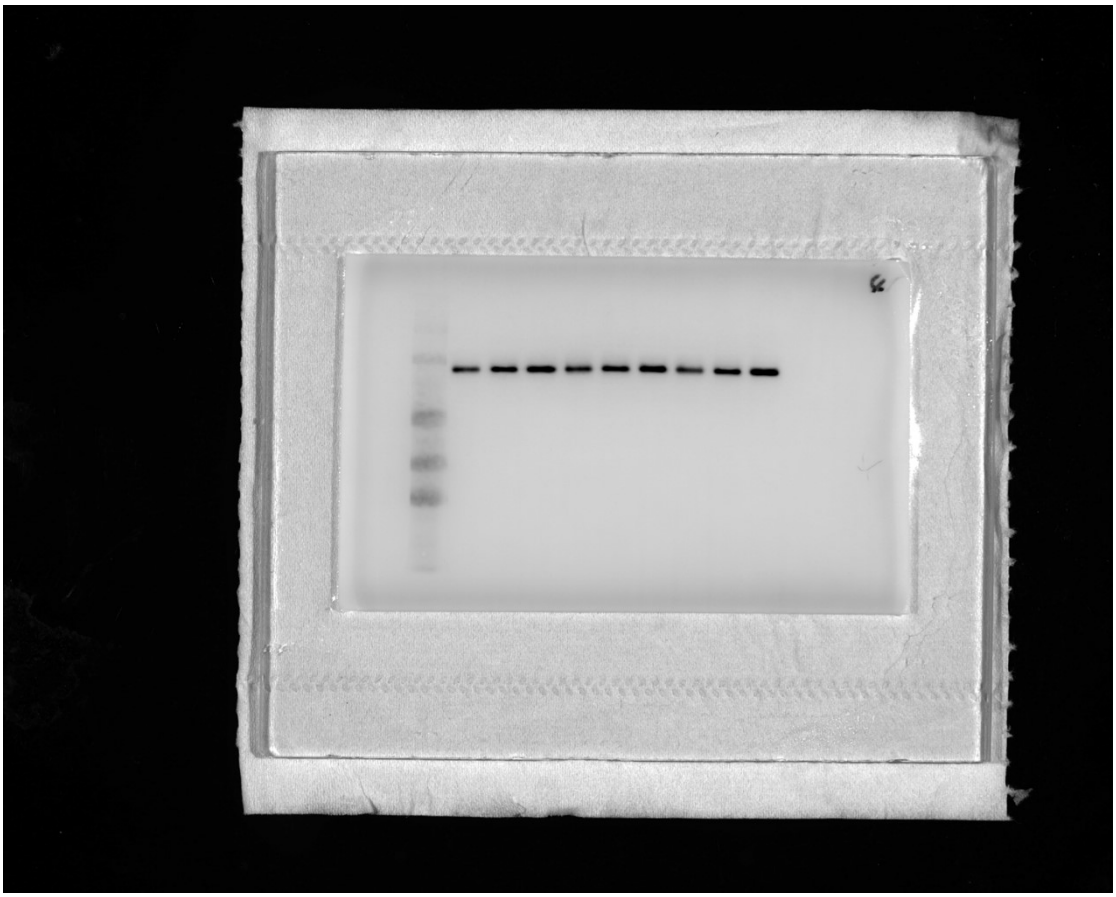

Materials and methods

I*n vivo assays*

SKO3 cancer cells were harvested and injected subcutaneously into the right flank of nude mice with 5×10^6 cells in 200 μL of serum-free medium. When the xenograft tumor growth to the volume about 1.0 cm^3, the mice were killed and the tumor tissue were cut into about 1.5 mm^3 small pieces, and then transplanted into the right flank of female nude mice, When tumors reach a volume of 0.09-0.10 cm^3 on all mice, the mice were randomized into vehicle control and treatment groups (n=6/group), received the following treatments: (a) control, 5.0% v/v DMSO/saline vehicle, (b) **tpy1Pt** at dose 5.0 mg/kg every two day (5.0% v/v DMSO/saline). The tumor volumes were determined every three days by measuring length (*l*) and width (*w*) and calculating volume, tumor volume and inhibition of tumor growth were calculated using formulas 1−3: [1−5]

Tumor volume: $V = (w^2\times l)/2$ (1)

The tumor relative increment rate: $T/C\ (\%) = T_{RTV}/C_{RTV}\times100\%$ (2)

inhibition of tumor growth: $IR(\%) = (W_c - W_t)/W_c\times100\%$ (3)

Where w and l mean the shorter and the longer diameter of the tumor respectively; T_{RTV} and C_{RTV} was the RTV of treated group and control group respectively. (RTV: relative tumor volume, $RTV= V_t /V_0$); W_t and W_c mean the average tumor weight of complex-treated and vehicle/controlled group respectively.

In addition, the SKO3 xenograft mouse models were purchased from Shanghai Lingchang Biotechnology Co., Ltd. (Shanghai, China, approval No. SCXK(Hu) 2018-0003). The animal procedures were approved by Nanjing Ramda Pharmaceutical Co., Ltd. (Jiangsu, China, approval No. SYXK(Su) 2022-0038). And all of the experimental procedures were carried out in accordance with the NIH Guidelines for

the Care and Use of Laboratory Animals. The animal experiments were approved by Nanjing Ramda Pharmaceutical Co., Ltd. (Jiangsu, China).

Statistical Analysis

The experiments have been repeated from three to five times, and the results obtained are presented as means ± standard deviation (SD). Significant changes were assesses by using Student's *t* test for unpaired data, and p values of <0.05 were considered significant.

Abbreviations

SD, standard deviation; TBS, Tris-HCl buffer; MTT, 3-(4,5-dimethylthiazol-2-yl)-2,5-diphenyltetrazolium bromide; TGI, tumor growth inhibition; PI, propidium iodide; MMP, mitochondrial membrane potential; JC-1, 5,5′,6,6′-tetrachloro-1,1′,3,3′-tetraethylbenzimidazolylcarbocyanine; IR, tumor growth inhibition rate.

References

[1] (a) Y. Lai, N. Lu, A. Ouyang, Q. Zhang, P. Zhang, Ferroptosis promotes sonodynamic therapy: a platinum(II)-indocyanine sonosensitizer, Chem. Sci. 13 (2022) 9921–9926. (b) X.-M. Liu, Z. Li, X.-R. He, R.-P. Liu, Z.-Y. Ma, X. Qiao, S.-Q. Wang, J.-Y. Xu, Dual-targeting of the aromatase binding domain of heme and androstenedione by Pt(IV) prodrugs: a new treatment for postmenopausal breast cancer, Inorg. Chem. Front. 9 (2022) 3470–3483. (c) Y. Li, S. Shi, S. Zhang, Z. Gan, X. Wang, X. Zhao, Y. Zhu, M. Cao, X. Wang, W. Li, ctc-[$Pt(NH_3)_2$(cinnamate)(valproate)Cl_2] is a highly potent and low-toxic triple action anticancer prodrug, Dalton Trans. 50 (2021) 11180–11188.

[2] (a) M. Uemura, K. Hiramoto, H. Yoneyama, S. Harusawa, S. Komeda,

Introduction of Fluorine into Antitumor-Active Dinuclear Platinum(II) Complexes Leads to Modulation of In Vivo Antitumor Activity in Mice, Inorg. Chem. 61 (2022) 12155−12164. (b) Y.-F. Wang, J.-X. Tang, Z.-Y. Mo, J. Li, F.-P. Liang, H.-H. Zou, The strong in vitro and vivo cytotoxicity of three new cobalt(II) complexes with 8-methoxyquinoline, Dalton Trans. 51 (2022) 8840–8847.

[3] (a) Y.-Q. Gu, W.-Y. Shen, Q.-Y. Yang, Z.-F. Chen, H. Liang, Ru(III) complexes with pyrazolopyrimidines as anticancer agents: bioactivities and the underlying mechanisms, Dalton Trans. 51 (2022) 1333–1343. (b) W.-Y. Shen, C.-P. Jia, A.-N. Mo, H. Liang, Z.-F. Chen, Chemodynamic therapy agents Cu(II) complexes of quinoline derivatives induced ER stress and mitochondria-mediated apoptosis in SK-OV-3 cells, Eur. J. Med. Chem. 223 (2021) 113636. (c) X. Huang, S. Hua, R. Huang, Z. Liu, S. Gou, Z. Wang, Z. Liao, H. Wang, Dual-targeting antitumor hybrids derived from Pt(IV) species and millepachine analogues, Eur. J. Med. Chem. 148 (2018) 1–25.

[4] (a) Z. Zhou, L.-Q. Du, X.-M. Huang, L.-G. Zhu, Q.-C. Wei, Q.-P. Qin, H. Bian, Novel glycosylation zinc(II)-cryptolepine complexes perturb mitophagy pathways and trigger cancer cell apoptosis and autophagy in SK-OV-3/DDP cells, Eur. J. Med. Chem. 243 (2022) 114743. (b) Z.-F. Wang, X.-F. Zhou, Q.-C. Wei, Q.-P. Qin, J.-X. Li, M.-X. Tan, S.-H. Zhang, Novel bifluorescent Zn(II)-cryptolepine-cyclen complexes trigger apoptosis induced by nuclear and mitochondrial DNA damage in cisplatin-resistant lung tumor cells, Eur. J. Med. Chem. 238 (2022) 114418. (c) S.-H. Zhang, Z.-F. Wang, H. Tan, Novel zinc(II)-curcumin molecular probes bearing berberine and jatrorrhizine derivatives as potential mitochondria-targeting anti-neoplastic drugs, Eur. J. Med. Chem.

243(2022) 114736. (d) L. Li, X. Huang, R. Huang, S. Gou, Z. Wang, H. Wang, Pt(IV) prodrugs containing microtubule inhibitors displayed potent antitumor activity and ability to overcome cisplatin resistance, Eur. J. Med. Chem. 156 (2018) 666–679. (e) Q.-P. Qin, Z.-Z. Wei, Z.-F. Wang, X.-L. Huang, M.-X. Tan, H.-H. Zou, H. Liang, Imaging and therapeutic applications of Zn(II)-cryptolepine–curcumin molecular probes in cell apoptosis detection and photodynamic therapy, Chem. Commun. 56 (2020) 3999–4002.

[5] Q.-P. Qin, Z.-F. Wang, S.-L. Wang, D.-M. Luo, B.-Q. Zou, P.-F. Yao, M.-X. Tan, H. Liang, In vitro and in vivo antitumor activities of three novel binuclear platinum(II) complexes with 4’-substituted-2,2’:6’,2’’-terpyridine ligands, Eur. J. Med. Chem. 170 (2019) 195−202.